GEOLOGIC NOTE

Deformation bands and their influence on fluid flow

Haakon Fossen and Arthur Bale

ABSTRACT

Deformation bands represent a common type of strain localization in deformed porous sandstones and occur as single structures, as clusters, and in fault damage zones. They show from zero to six orders of magnitude reduction in permeability and may therefore potentially affect fluid flow. We here present mathematical calculations indicating that uncommonly high permeability contrasts and/or exceptionally high band concentrations are required for deformation bands to significantly affect production rate. We also present field observations showing rapid variations in porosity and permeability along deformation bands and deformation-band zones alike. Furthermore, many paleofluid fronts seen in the field are unaffected or only gently affected by deformation bands. Together, these calculations and observations suggest that their function during reservoir production is small or negligible in most cases. Structural complications caused by subseismic faulting and complex fault anatomy are more likely to cause production problems, in addition to stratigraphic and diagenetic effects. Nevertheless, the arrangement and orientation of deformation bands may have an effect on the flow pattern and reservoir sweep. In cases where deformation bands do cause production problems, it may be possible to resolve these by means of hydraulic fracturing.

INTRODUCTION

In porous rocks and sediments, subseismic brittle deformation is largely expressed by a special type of small, faultlike structures referred to as deformation bands (see Fossen et al., 2007, for a review). Deformation bands (Figure 1) are found in most siliciclastic reservoir sandstones, where they tend to have lower permeability

Manuscript received December 21, 2006; provisional acceptance February 28, 2007; revised manuscript received May 4, 2007; final acceptance July 30, 2007.
DOI:10.1306/07300706146

AUTHORS

Haakon Fossen ~ *Department of Earth Science, University of Bergen, Allégaten 41, N-5007 Bergen, Norway; Haakon.Fossen@geo.uib.no*

Haakon Fossen received his Cand. Scient. (M.Sc. equivalent) degree from the University of Bergen (1986) and his Ph.D. in structural geology from the University of Minnesota (1992). He joined Statoil in 1986 and, since 1996, has been a professor in structural geology at the University of Bergen. His scientific interests cover the evolution and collapse of mountain ranges, the structure of rift basins, and petroleum-related deformation structures at various scales.

Arthur Bale ~ *Statoil, Sandslihaugen 30, 5020 Bergen, Norway; ARBA@statoil.com*

Arthur Bale is a propped fracturing specialist and production engineering supervisor with Statoil in Bergen, Norway. Bale has held several assignments with Statoil, including technical supervisor and advisor for rock mechanics and petrophysics. Prior to joining Statoil in 1984, he worked with Amoco as a reservoir engineer in Norway and as a research engineer in Tulsa, Oklahoma. Bale holds an M.Sc. degree in petroleum engineering from the Norwegian Institute of Technology in Trondheim, Norway. He has authored and coauthored numerous Society of Petroleum Engineers (SPE) papers and served on SPE committees.

ACKNOWLEDGEMENTS

Thanks are due to Statoil for financial support and stimulating field trips over the last 15 yr of studying faults and deformation bands in the field. Very helpful referee comments were provided by R. K. Davies, Q. Fisher, and A. Lacazette.

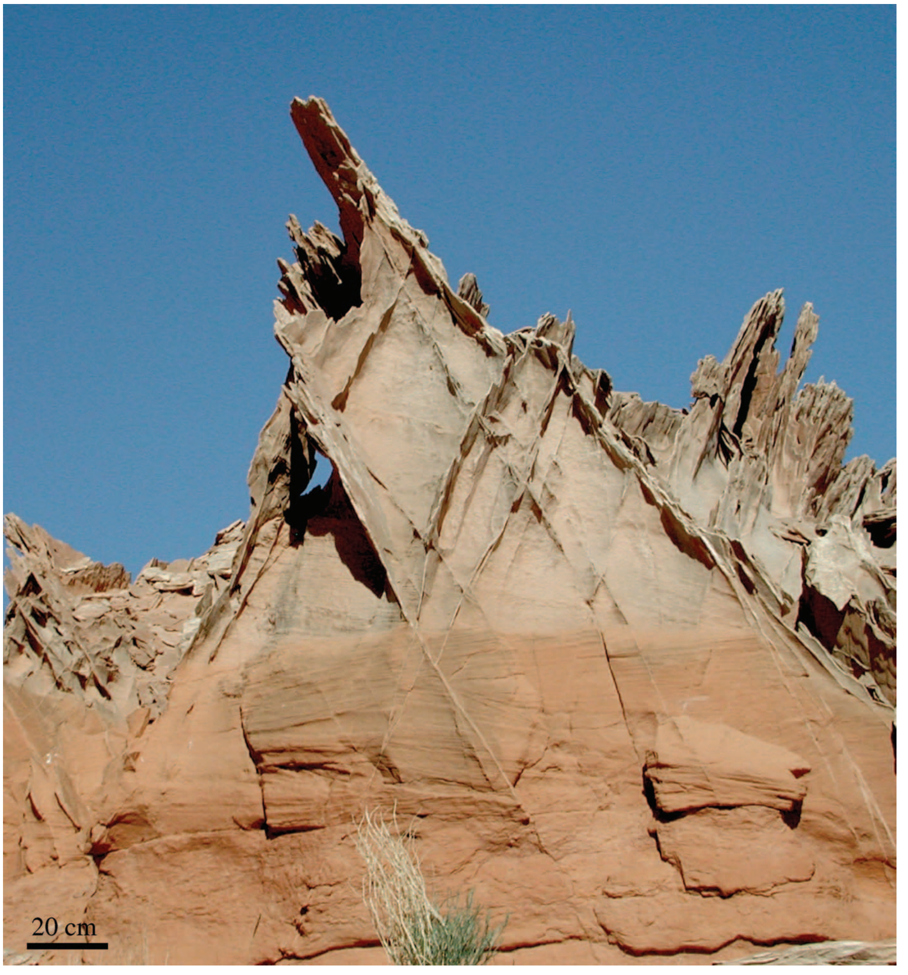

Figure 1. Deformation bands in the Entrada Sandstone, Utah. Note the conjugate arrangement of the bands and the way they disappear downward as they enter the low-porosity siltstone. The highly permeable upper layer has been bleached by reducing fluids. The paleogroundwater flow was controlled by lithology, not by deformation bands.

than their host rocks (e.g., Pittman, 1981; Jamison and Stearns, 1982; Antonellini and Aydin, 1994; Knipe et al., 1997; Gibson, 1998; Fisher and Knipe, 2001; Lothe et al., 2002; Shipton et al., 2002). Thus, they are considered by many to baffle the flow of fluids during oil production (e.g., Knipe et al., 1997; Gibson, 1998) and to act as seals for hydrocarbon accumulations (e.g., Ogilvie and Glover, 2001).

In practice, proving that deformation bands have a significant influence on fluid flow in petroleum reservoirs is difficult. This is related to our limited knowledge of subseismic structures in reservoirs: where do they occur, and what are their petrophysical properties? Are they thick or numerous enough to have an effect? Are they distributed and arranged in such a way that they perturb fluid flow? Several ways can answer these questions. We will discuss here the effect of deformation bands on fluid flow in the light of mathematical calculations, fluid-flow simulations, petrophysical measurements, and field observations.

FAULT ANATOMY

At subseismic resolution, a fault is generally defined as a planar or zonal structure across which appreciable (meter-scale or more) shear displacement discontinuity occurs (e.g., Billings, 1972, p. 174). Faults are sometimes considered as planes or surfaces (e.g., Hobbs et al., 1976), also called slip planes or shear fractures. In detail, most faults have a certain thickness and consist of cataclasite, breccia, or sheared layers of weak lithologies. This zone of highly sheared and/or intensely fractured rocks is now commonly referred to as the fault core (Caine et al., 1996). The fault core thickness generally varies with the amount of fault offset, from a few millimeters or centimeters for subseismic faults up to 1 dm (4 in.) or even several meters for kilometer-scale faults (Figure 2). The sealing property of a fault is mostly controlled by the petrophysical properties, continuity, and thickness of the fault core. In particular, smearing of shale layers within the core is important.

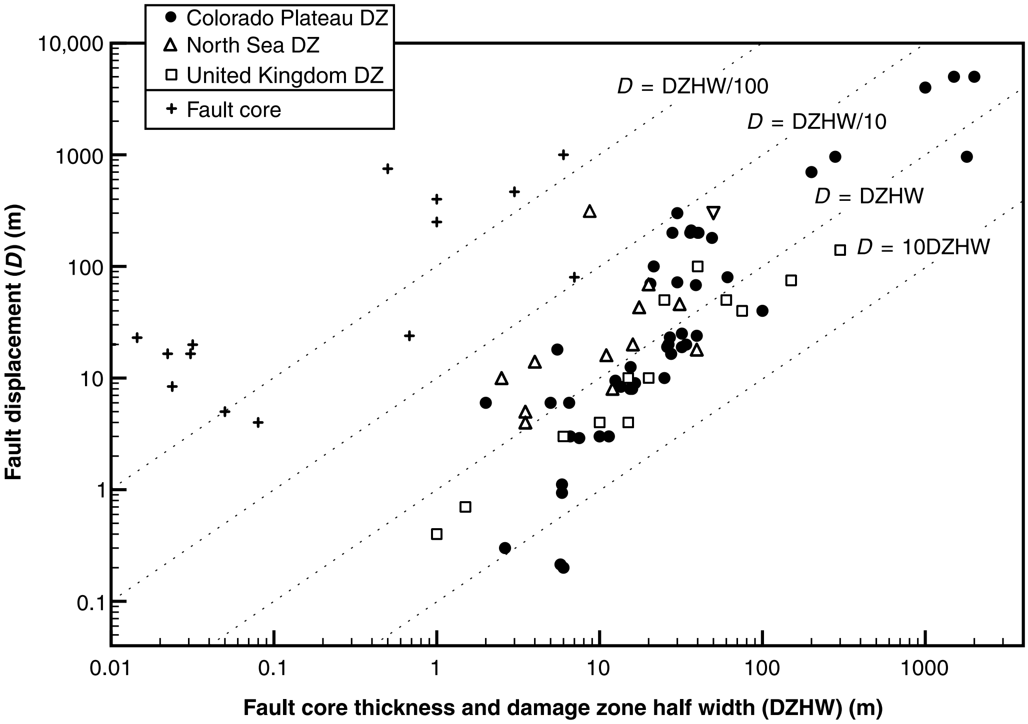

Figure 2. Damage zone half-width for faults in sandstones, plotted against fault displacement. Fault core data from the same area are indicated. Data are from Knott et al. (1996), Hesthammer and Fossen (2001), Shipton et al. (2005), and own observations from the Colorado Plateau. DZ = damage zone.

In this work, we will focus on the zone (volume in three dimensions) of brittle deformation around the fault core, known as the fault damage zone (Peacock et al., 2000). Statistically, a damage zone is wider than its fault core by about two orders of magnitude (Figure 2). As indicated in Figure 2, the displacement of a fault is related to the width of its damage zone. However, large and rapid variations in damage zone thickness occur along most faults, and estimating damage zone width from displacement is therefore associated with great uncertainty.

In low-porosity rocks, such as crystalline rocks and many limestones, the brittle deformation structures in the damage zone are shear fractures (slip surfaces) and/or extension fractures. However, in highly porous sandstone reservoirs, damage zones are dominated by a somewhat different type of structure known as deformation bands (see section below).

The damage zone and its structure elements represent a petrophysical anomaly in any reservoir rock as compared to the pristine host rock inasmuch as the damage zone structures alter the permeability structure of the rock. In general, damage zone fractures enhance permeability along faults in low-porosity and nonporous rocks, whereas damage zones represent volumes of reduced permeability in highly porous rocks. Below, we will focus on highly porous reservoir rocks and the deformation bands that populate damage zones in such lithologies.

CHARACTERISTICS OF DEFORMATION BANDS

Deformation bands are millimeter-thick tabular zones of localized strain. They deviate from regular fractures by their lack of a single, continuous slip surface. For this reason, they do not share all of the properties of regular fractures. For instance, they do not necessarily represent mechanically weak structures or zones of reduced cohesion, but are commonly found to be stronger and more cohesive than their host rock. Furthermore, they tend to involve reduction of porosity and permeability, whereas faults and fractures involve an increase in porosity and permeability. Deformation bands also tend to be thicker than slip surfaces of comparable displacements. Individual deformation bands in sandstones typically have thicknesses of about 1 mm (0.04 in.). Deformation-band clusters are wider, commonly in the order of centimeters or decimeters (Figure 3).

Most deformation bands show a dominant component of shear displacement. The shear displacement is small, typically a few millimeters or centimeters across single bands. A minor component of compaction across the bands is common because they lose porosity during granular flow, fracturing, and/or grain-boundary solution. Less commonly, pure compaction bands are found (Mollema and Antonellini, 1996), and rare examples of dilation bands also exist (Du Bernard et al., 2002).

Figure 3. Thickness-displacement data for deformation bands (single bands and clusters).

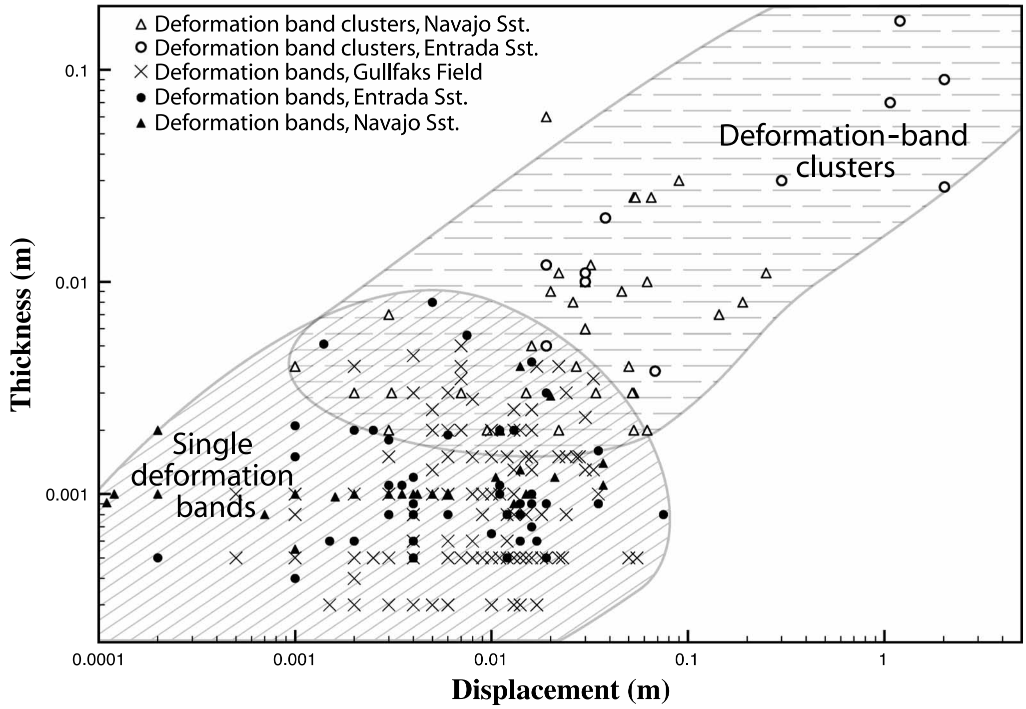

Deformation bands are confined to highly porous media, notably sandstones with porosity in excess of approximately 15%. In sandstones, they occur as single structures, as clusters, and in fault damage zones. This occurrence suggests that deformation bands form prior to fault formation, i.e., that faults in sandstones form by faulting of precursory deformation-band clusters (Aydin and Johnson, 1978). Faulting of deformation-band clusters seems to occur by the growth of patches of slip surfaces in the low-porosity parts of deformation-band clusters (Shipton and Cowie, 2003). The patches connect and develop into a continuous slip surface or fault. The implication of this model is that faults in highly porous sandstones are always surrounded by deformation bands, i.e., the fault damage zone consists of deformation bands. However, it also implies that deformation bands can exist as single bands or deformation-band clusters away from faults. A comprehensive core study from the North Sea Gullfaks field (Hesthammer and Fossen, 2001) showed that almost 30% of the deformation bands in this oil field occur away from faults.

Several types of deformation bands exist, which can be classified into three groups based on host rock mineralogy and deformation mechanism (Fossen et al., 2007). One type is disaggregation bands, where grains are reorganized by rolling and sliding only (noncataclastic granular flow). The grains remain intact, although the grain reorganization can lead to dilation or, more commonly, compaction. A special variety of disaggregation band that occurs in phyllosilicate-bearing sandstones is known as (framework) phyllosilicate bands (Knipe et al., 1997). In these bands, phyllosilicates such as mica and clay are mechanically realigned to form a fabric parallel to the band.

The other main kind of deformation band is termed cataclastic bands (Aydin and Johnson, 1978). In such bands, grains are crushed (cataclasis), and the grain size consequently reduced. Moreover, cementation and dissolution at grain-grain contact points can reduce porosity in any type of deformation band. Such effects can occur after the band is formed, particularly at temperatures in excess of about 90°C (Walderhaug, 1996). Deformation bands may be preferentially cemented because of their fresh grain surfaces formed during frictional grain sliding and comminution.

Many factors influence the deformation mechanism and, hence, the type of deformation band formed, including mineralogy, grain size, grain shape, grain sorting, degree and type of cementation, porosity, and confining pressure. Whereas the composite effects of these factors are not completely understood, it is generally seen that disaggregation bands preferentially form at shallow depths (<1 km; <0.6 mi) in weakly consolidated sandstones, whereas cataclastic bands tend to form in more deeply buried sandstones (Fossen et al., 2007).

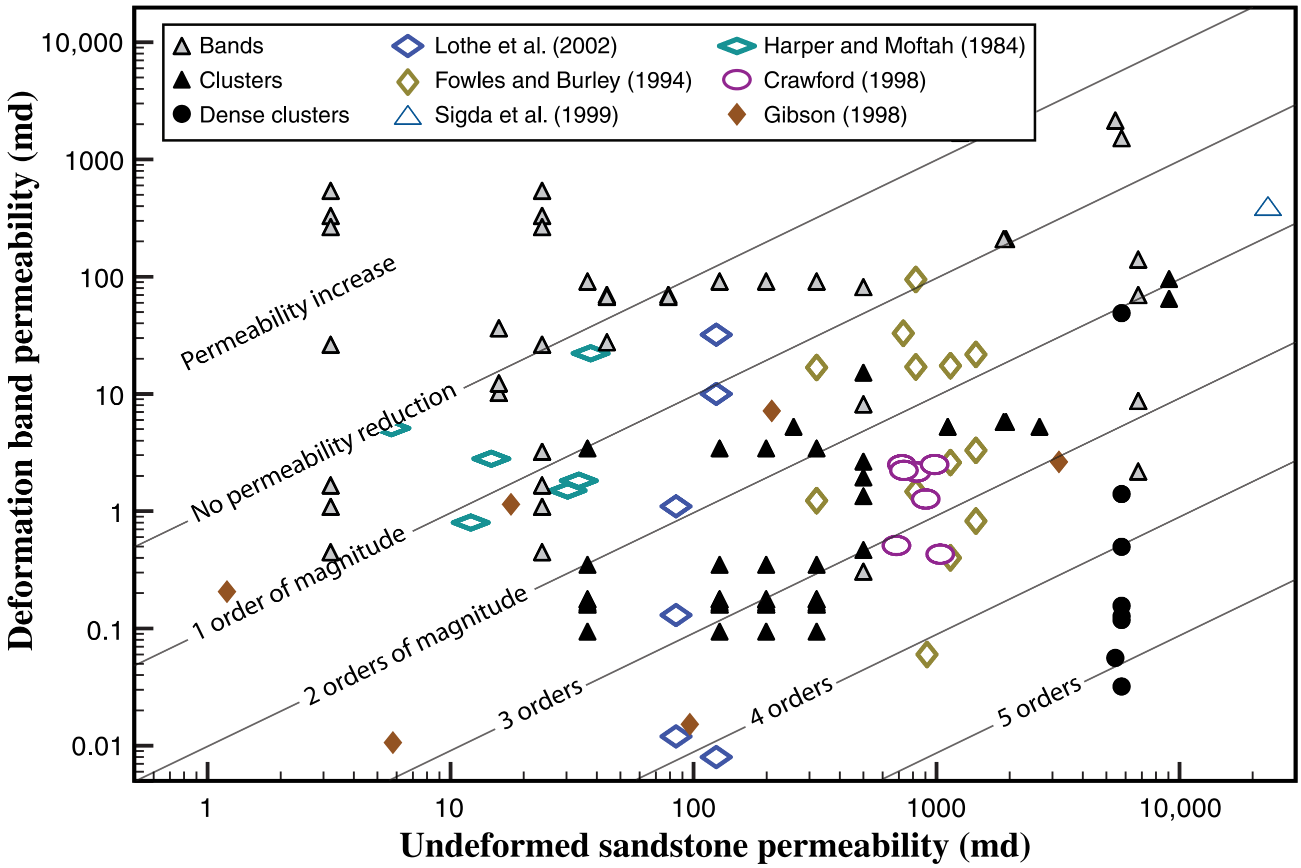

Figure 4. Permeability of host rock plotted against that of deformation bands as measured from plugs drilled perpendicular to the bands. Most of the bands are cataclastic deformation bands. Our data, mostly from southern Utah, are separated into single bands, clusters, and dense clusters of deformation bands. Previously published data are shown for comparison (not separated into single bands and clusters).

PETROPHYSICAL PROPERTIES

Several publications report on laboratory measurements of permeability across single or clustered deformation bands in reservoir-type clastic sediments (Pittman, 1981; Jamison and Stearns, 1982; Harper and Moftah, 1985; Knott, 1993; Antonellini and Aydin, 1994; Gibson, 1994, 1998; Mollema and Antonellini, 1996; Knipe et al., 1997; Crawford, 1998; Antonellini et al., 1999; Fisher and Knipe, 2001; Jourde et al., 2002; Shipton et al., 2002; Flodin et al., 2005). A review of the data together with new, unpublished measurements (Figure 4) shows reduction in permeability across deformation bands by up to five to six orders of magnitude in extreme cases, whereas the average permeability reduction is about two to three orders of magnitude (e.g., Taylor and Pollard, 2000).

It is not always clear from published data sources whether permeability has been measured across single or multiple bands. Our own data show that the difference is significant. Although single cataclastic deformation bands from highly permeable (>1 d) Jurassic sandstones of the Colorado Plateau show one to two orders of magnitude of permeability reduction, cluster zones with densely packed deformation bands from the same layer show reductions of about five orders of magnitude. To explore the implications of these numbers in a flow situation, a theoretical treatment is given below.

THEORETICAL CONSIDERATIONS

From the above, the highest concentrations of deformation bands in a faulted high-porosity sandstone reservoir clearly occur in the fault damage zone, i.e., close to the faults. We will consider here a simple but realistic example that includes a producer and an injector

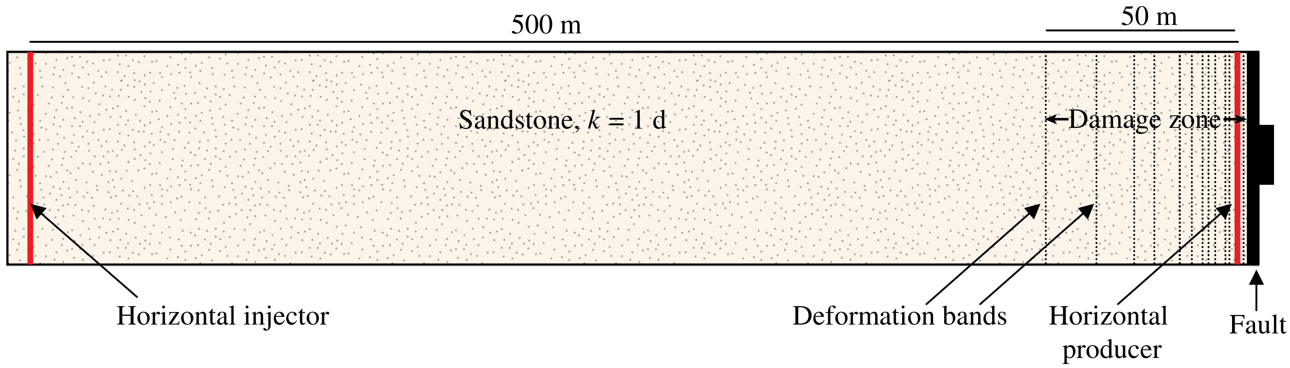

Figure 5. Schematic bird's eye view of a production situation in a sandstone reservoir. A producer is located in a damage zone close to the fault, and an injector is located outside of the damage zone. See text and Appendices for discussion.

(Figure 5) based on the mathematical framework describing linear, single-phase flow in porous media across low-permeability zones such as deformation bands and deformation-band zones (presented in Appendices 1 and 2). This calculation example does not represent an attempt to estimate the reduction in production rate because well production will be dependent on several variables not considered here, including stratigraphic thickness, characteristics of the nearby fault, wellbore radius, perforated interval, etc. This type of analysis would probably require the use of a reservoir simulator because a simple analytical solution is not readily available for the subject drainage pattern. The purpose of the calculation example presented here is simply to show the fractional reduction in productivity as a result of reduced average permeability between the injector and producer, as caused by the presence of deformation bands. Productivity is linearly related to the effective or average permeability between an injector and producer, regardless of boundary effects (steady-state or pseudo–steady-state pressure conditions or distances to reservoir boundaries and wellbore geometry). Hence, the results are not affected by the presence of the injector, which was included to make the example analogous to the steady-state pressure conditions referred to in Appendix 2.

Figure 5 represents a typical sandstone reservoir with a horizontal injector placed 500 m (1640 ft) from a fault where a horizontal producer is placed in a fault damage zone very close to (say, 0.5 m [1.64 ft] from) the fault. Between the producer and the injector is a zone of deformation bands in a 50-m (164-ft)-wide zone from the fault. The permeability, k, in the pristine host rock is taken to be 1 d (1000 md). We emphasize that the example is linear, meaning that the wells are fully perforated and deformation bands are considered as infinitely long, extending across the entire sandstone layer with constant thickness and properties. Natural deviations from these conditions, including the effect from the nearby fault, are discussed in the sections below.

We want to use realistic values for the thicknesses and petrophysical properties of deformation bands before evaluating their cumulative effect on fluid flow. The average deformation-band thickness is about 1 mm (0.04 in.) (Figure 3). Clusters of bands contain multiple deformation bands, and their cumulative thickness reaches a couple of decimeters in thickness. The linear trend for cluster zones in Figure 3 is consistent with the model that they grow by forming new deformation bands along preexisting one(s). Hence, the thickness of a deformation-band cluster zone can be modeled by multiplying the number of bands it contains with the average band thickness. The same can be done for fault damage zones: their influence on fluid flow is related to the permeability of each band and the sum of their thicknesses (see Appendix 2).

Figure 6 is a dimensionless plot where the fractional reduction in flow rate or productivity, in the following referred to as flow efficiency (FE), is plotted against dimensionless values of k/k_{DB}. The value k_{DB} represents the permeability within (or across) the deformation bands, whereas k is the host rock permeability.

Note that although Figure 5 shows a gradual increase in deformation-band density toward the fault (which is the case for most fault damage zones), the mathematical framework (equation 11) shows that the internal position and distribution of the bands in this setting is of no importance. The average permeability, k_A, between the injector and the producer depends on k/k_{DB} and the product between the number of bands it has to cross and their thickness ($n \times t_{DB}$). Thus, Figure 6 becomes universal and independent of the absolute

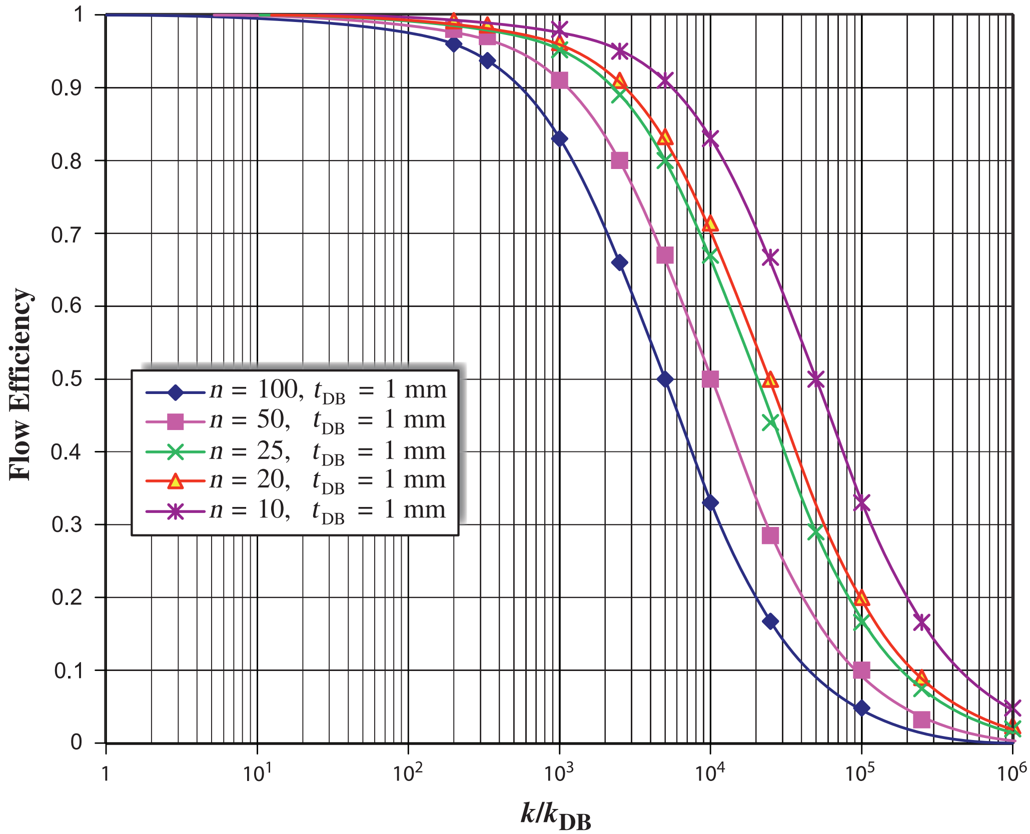

Figure 6. Flow efficiency versus host rock and deformation-band permeability ratio (k/k_{DB}) based on the mathematical framework presented in the text and Appendices and the situation illustrated in Figure 5. t_{DB} = deformation band thickness.

value of k, although the values for flow efficiency, to a minor extent, depend on the distance L between the injector and the producer. However, variations in L have small consequences for small values of k/k_{DB} ($<10^3$) and realistic numbers and characteristics of deformation bands.

The graph (Figure 6) indicates that the direct effect of deformation bands with a permeability contrast of three orders of magnitude or less ($k/k_{DB} \leq 10^3$) on fluid flow is small or negligible. For $k/k_{DB} = 10^3$, the reduction in productivity in the producer (Figure 5) can be seen from Figure 6 to be 17% (flow efficiency = 0.83) for a cluster or damage zone containing 100 bands (t_{DB} = 0.001 m [0.003 ft]). For rare cases where higher contrasts in permeability and/or higher densities of deformation bands are present, the effect will increase. These findings are in agreement with those of Manzocchi et al. (1998) and Walsh et al. (1998).

DEFORMATION-BAND CONTINUITY

The theoretical considerations presented above suggest that the (cumulative) thickness and the permeability of deformation bands pose key controls on the function of deformation bands during reservoir production. However, the continuity of the bands in the vertical and horizontal direction can be equally important. It is essential to realize that most laboratory measurements of permeability rely on inch-thick plugs drilled from outcrops, field samples, or cores. These measurements, therefore, do not consider any variations that may exist along the bands outside the volume covered by the plug. The same is the case with the one-dimensional considerations presented in the section above.

Field studies show that many deformation bands and cluster zones are laterally extensive structures. In fact, the uncommonly low displacement-length ratios of cataclastic deformation bands suggest that they are longer than one would expect from their limited displacement values, as compared to the established displacement-length relation for ordinary faults (Fossen and Hesthammer, 1997). This fact increases their ability to perturb fluid flow. However, they are restricted to highly porous layers and are commonly seen to become thinner, decrease in number, or even vanish at layer boundaries across which porosity decreases, sorting becomes poorer, and/or grain size goes down (Schultz and Fossen, 2002) (Figure 1).

Detailed field investigations also show that although many bands and zones are continuous over considerable

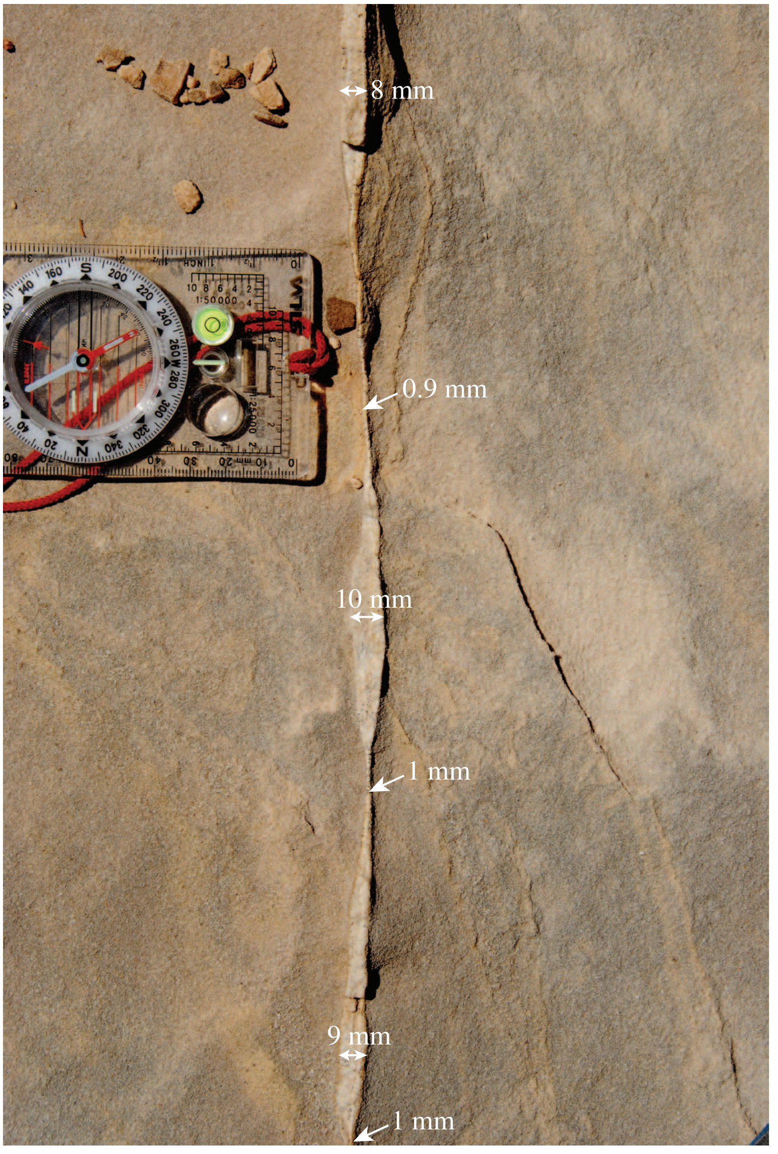

Figure 7. Deformation band in the Entrada Sandstone showing rapid changes in thickness. San Rafael Desert, Utah.

distances, their thickness and internal permeability structure may change abruptly. Thickness variations along single bands can be seen to be from 1 cm (0.4 in.) down to less than 1 mm (0.04 in.) even over distances of only some centimeters (Figure 7). These variations occur in both the vertical and horizontal direction without any obvious relation to lithology.

The thinnest parts of a deformation band represent points of potential leakage and deserve closer attention. Thin-section studies show that there can be rapid variations in porosity and permeability within these thin parts of the bands. As shown in the examples from the Nubian Sandstone (Sinai) and the Entrada Sandstone (Utah) (Figure 8), porosity is greatly reduced on the left-hand side of the pictures because of cataclasis and some solution-related compaction. However, on the right-hand side, the bands get thinner, and the porosity within the bands is high. Although the left-hand parts of the bands reduce permeability by several orders of magnitude compared to the host rock, the reduction on the other side of the field of view is negligible. Clearly, such weak points control the pressure difference that can be maintained across a deformation band.

Deformation-band clusters, which may contain hundreds of deformation bands in some cases, show similar variations in thickness. Figure 9 shows how a decimeter-thick cluster zone in the Entrada Sandstone pinches into a centimeter-thin zone over a short distance. Undoubtedly, such variations reduce the ability of low-permeability deformation-band clusters to stop fluid flow in a reservoir

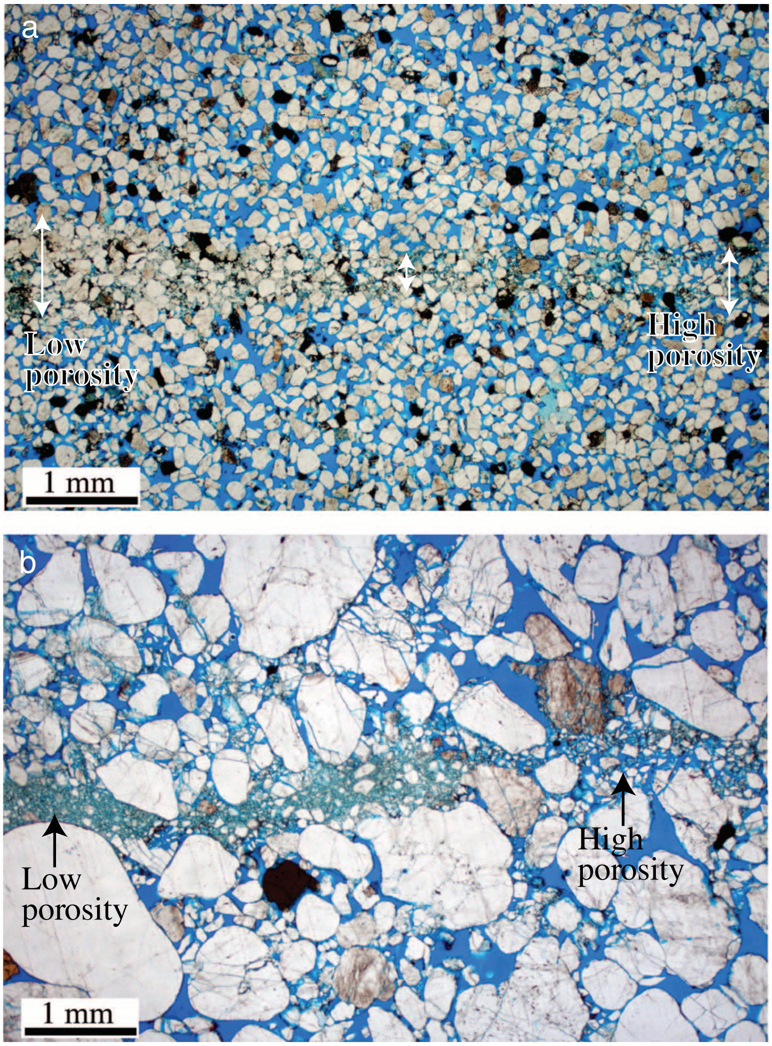

Figure 8. Photomicrographs of two deformation bands, both showing rapid increase in porosity from the left to the right. Such variations decrease the effect of such structures to reduce permeability in a reservoir. (a) Entrada Sandstone, San Rafael Desert. (b) Nubian Sandstone, Tayiba Mines, Sinai.

setting. The tortuous paths involved may, however, slow down fluid flow and negatively influence sweep efficiency during water injection.

FIELD OBSERVATIONS OF PALEOFLUID FLOW

Evidence of paleofluid flow can be found in sandstones that have since been uplifted and exposed. Flow of groundwater leaves or removes mineral grain coatings, and paleofluid fronts show up in the field as colored bands or interfaces between differently colored parts of sandstone layers. A well-known example is the bleaching of hematite-stained sand grains of porous sandstones by chemically reducing fluids. This effect is seen in many porous sandstone formations, such as the Nubian Sandstone of the Gulf of Suez and the Navajo and Entrada sandstones of the Colorado Plateau (e.g., Beitler et al., 2003). In many cases, reducing fluids have preferentially bleached highly permeable sandstone laminas or beds in less permeable but still reservoir-quality sandstones. In detail, fluid flow can be seen to be sensitive to small porosity and permeability changes within porous sandstone units. Knowing that most deformation bands have lower porosity and permeability than their host rocks, one would expect them to show a similar influence on fluid flow in sandstones.

Bleaching along the Moab fault in southeastern Utah is probably caused by hydrocarbons (Garden et al., 2001) in addition to reducing saline groundwater (Chan et al., 2001). Chan et al. (2000) used C, O, and Sr isotopic data, fluid inclusions, and geohydrologic reconstructions to show that reducing, saline fluids transmitted on fault systems mixed with oxygenated groundwater to precipitate the mineralization. Solum et al. (2005) estimated the latest period of major faulting to have occurred at about 60 Ma. Chan et al. (2001) presented

Figure 9. Deformation-band cluster in the Entrada Sandstone showing rapid changes in thickness. San Rafael Desert, Utah.

age estimates of 25–20 Ma for the mineralization, pointing at a possible relation with the Colorado Plateau uplift or magmatic activity in the nearby La Sal Mountains area. These ages suggest that the bleaching and diagenetic alterations occurred after the formation of the deformation bands in the Moab area.

In none of the observed cases can deformation bands be shown to have had any visible effect on the reduction fronts (Figures 10 and 11). The type of deformation bands studied in the Entrada and Navajo sandstones is mostly cataclastic in the dune deposits and disaggregation in the interdune deposits. Cataclastic deformation bands in this area show permeability reductions of up to three orders of magnitude (Antonellini and Aydin, 1994), but still have no visible effect on fluid flow. This is the case for both single bands and the network zones (Figure 10) closer to the fault core. However, staining patterns have not yet been found around dense deformation-band clusters of the type shown in Figure 9; so their effect on the paleofluid flow is unknown. Another example from the Nubian Sandstone of the western Sinai Peninsula is also shown in Figure 11. Again, cataclastic single deformation bands had no apparent influence on fluid flow. These observations agree with the theoretical considerations outlined above and the variations in deformation-band thickness and permeability structure, as explored in the previous section (Figures 7–9). However, refractions of diagenetic alteration fronts by deformation bands have been reported from the Aztec Sandstone in the Valley of Fire, Nevada (Taylor and Pollard, 2000; Eichhubl et al., 2004), indicating that deformation bands can have some influence on fluid flow in a certain situation.

An important factor in these considerations is the time it took for fluids to remove or redeposit iron oxides and other minerals. The time aspect likely involved is more similar to that of oil migration than the short time involved in the production of hydrocarbon reservoir. Hence, although fluids manage to pass through deformation bands given thousands of years or more, this is no proof that deformation bands have no influence on fluid flow in a production setting. Nevertheless, it does illustrate that many low-porosity deformation bands are neglected by migrating fluids in reservoir sandstone. The reason for these observations may be low band connectivity (so that fluids are free to flow around and between bands), low thicknesses of deformation bands, variations in thickness and permeability along the bands, or simply that the physical properties of the deformation bands are not different enough from those of the host rock to stop fluid flow across them. It has not been possible to favor one explanation based on the paleofluid-related field data alone.

DISCUSSION

We have shown that for deformation bands and deformation-band clusters to effectively reduce fluid flow in a sandstone reservoir, their permeability must be much lower than the host rock permeability, and their cumulative thickness must be higher than what is found in many reservoirs. The considerations presented here are based on single-phase flow, which means that the conclusions may not be directly transferred to two-phase or multiphase flow systems. Deformation bands may have a more negative impact on fluid flow in water-wet reservoirs than predicted from the theoretical considerations in this work. In theory, deformation bands will behave as total barriers to hydrocarbon flow until the

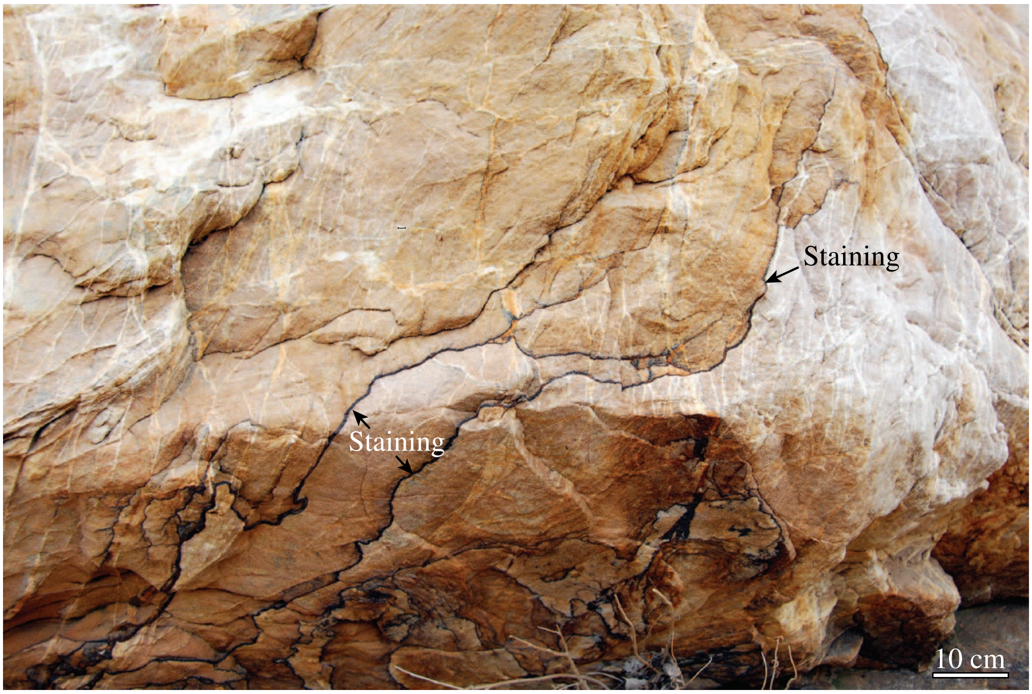

Figure 10. Iron oxide staining created by flowing groundwater. The black oxide seams indicate paleofluid fronts that appear to ignore the network of deformation bands in this outcrop of the Navajo Sandstone.

buoyancy force in the hydrocarbon column is sufficient to overcome the capillary entry pressure of the band. Once the entry pressure has been overcome, fluid flow will be controlled by its relative permeability characteristics (Fisher and Knipe, 2001).

Capillary forces dominate at low hydrocarbon saturations, i.e., near the base of the oil column. In this situation, water-wet deformation bands are likely to have higher permeability contrast with the host rock than the single-phase case discussed above and in the Appendices. This discrepancy decreases with increasing hydrocarbon saturation; for high hydrocarbon saturations, the nonwetting-phase permeability contrast is likely to approach that of a single-phase situation (Fisher and Knipe, 2001). This means that deformation bands may have a stronger influence on fluid flow toward the end of the production history of a well or field. However, the saturation distribution or anomalous capillary pressure inside a deformation band will be governed by the small thickness of the band (relative to the thickness of adjacent pristine rock) instead of the height above the free-water level. Hence, the saturation profile inside thin deformation bands may not differ significantly from the characteristics found inside the adjacent high-porosity and high-permeability host rock. If not true, their skin or detrimental impact on fluid flow would normally not be noticeable because of the small thickness of the deformation band. In many ways, this is analogous to fluids flowing from a hydraulic fracture in a reservoir sandstone through a zone where permeability has been damaged by the gels used during the hydraulic fracturing operations. In this case, linear flow is related to both the thickness of the zone of damage (analogous to the thickness of the deformation band) and also the characteristics of the fluids inside the zone (band). Mathematical considerations of such cases substantiate the numbers shown in Figure 6. These analytical solutions also suggest that the thickness, instead of realistic effective permeabilities of the damaged zone (governed by reduced absolute permeability) occasioned by crushed grains, relative permeability, and also capillary

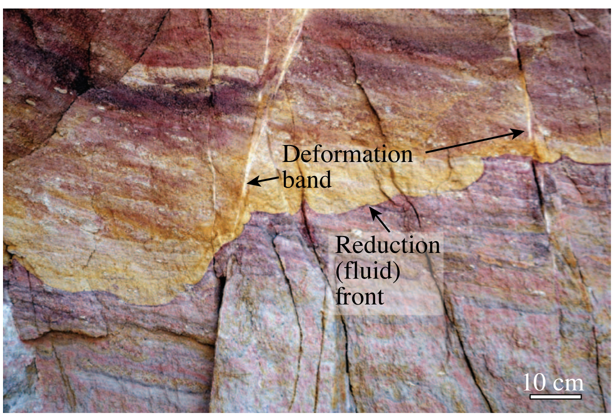

Figure 11. Paleofluid front in the Nubian Sandstone, unaffected by single or paired deformation bands. The fact that the fronts are not offset shows that they are younger than the bands.

pressure effects control flow across the damaged zone (Bale et al., 2001).

Regardless of the complications imposed by multiphase flow, we have demonstrated that deformation bands and clusters show rapid changes in both thickness and permeability, reducing their function as barriers to fluid flow. On top of this comes the limited connectivity of these structures in three dimensions. All together, these considerations indicate that deformation bands are unlikely to represent significant fluid-flow barriers during migration and production-injection in most cases, as suggested by the field observations of paleofluid flow.

Deformation bands have been found in most if not every faulted high-porosity sandstone reservoir where relevant core material is available. In the North Sea Gullfaks field, more than 4000 deformation bands have been identified in the cores, most of them located in fault damage zones (Hesthammer and Fossen, 2001). None of the data from the more than 200 Gullfaks injection and production wells have proved that deformation bands reduce productivity, although several are located very close to seismically resolvable faults. In general, only a few published examples exist where deformation bands are thought to reduce well performance. One is from the Nubian Sandstone of the Ras Budran oil field in the Gulf of Suez (Harper and Moftah, 1985). The cataclastic deformation bands encountered in this reservoir formed at depths of 1.5 km (0.9 mi) or more and involve reductions in permeability. However, the reported k/k_{DB} values are less than two orders of magnitude (Harper and Moftah, 1985) and, therefore, unlikely to reduce well productivity by any significant amount, according to the theoretical considerations discussed above and in the Appendices.

In another example, Hesthammer et al. (2002) suggest that post-tectonic cementation of deformation bands may explain low performance of the Gullfaks Sør reservoir in the North Sea. However, the limited cumulative thickness of deformation bands in the Gullfaks area damage zones and clusters (typically some tens of bands across each zone; Hesthammer and Fossen, 2001), together with the limited likelihood of forming spatially continuous post-tectonic selective quartz overgrowth structures, suggests that other explanations should be considered. Such effects include porosity and permeability reduction through general reservoir cementation and dissolution and, in particular, subseismic faults and fault complexities.

Having argued for a limited effect of deformation bands on well performance in most sandstone reservoirs, the mesoscopic petrophysical anisotropy imposed by deformation bands on the reservoir deserves some attention. This anisotropy is controlled by the structural arrangement of deformation bands along faults (Manzocchi et al., 1998). Field studies (Fossen et al., 2005; Johansen and Fossen, in press) and core analyses (Hesthammer et al., 2000) show that although deformation-band orientations may be complex, two sets tend to dominate. The two sets strike subparallel to the fault but dip in opposite directions, as shown in Figures 1 and 12. This conjugate arrangement may cause fluid flow in the reservoir to bypass and leave behind hydrocarbons in the fault damage zone in the same way low-permeability layers in a sandstone sequence may be poorly swept during water flooding. Hence, perforating the damage zone by placing injection or production wells amidst the deformation bands will develop a pressure profile inside the damage zone, which, in turn, will change the streamline potentials and, thus, improve reservoir sweep.

Reduced injectivity or productivity in wells located very close to a major fault can be explained by unexpected fault zone complications. The fault zone may consist of several downfaulted and partly isolated reservoir blocks, which will cause a rapid near-wellbore pressure increase in injectors (or pressure loss in producers). Even a fairly simple fault may cause reduction in productivity and injectivity for adjacent wells because of the near-wellbore reservoir boundary represented by the fault. The general steady-state flow equation (productivity index, PI, for a production well or injectivity index, II, for an injection well) is affected by the reservoir boundaries or Dietz shape factor, C_A (Dietz, 1965), as shown by the identity (e.g., Dake, 1994)

$$\mathrm{PI} = \mathrm{II} = \frac{q}{p_e - p_{wf}} = \frac{2\pi kh}{B\mu\left(\frac{1}{2}\ln\frac{16A}{e^{\gamma}C_A r_w^2}\right)} \tag{1}$$

where q is the production or injection rate, p_e is the reservoir pressure at the reservoir boundary, p_{wf} is the wellbore flowing pressure, k is the effective permeability, h represents the reservoir thickness, B is the oil-volume factor, μ is the fluid viscosity, A is the drainage area, e^{γ} equals $e^{0.57721} = 1.781$, and r_w is the wellbore radius.

The dimensionless (reservoir) shape factor may severely impact the deliverability of a production or injection well; although the Dietz shape factor for a well placed in the middle of a circular reservoir will be 31.6, the corresponding value can be less than 0.1 for a well placed in the corner of an equilateral triangle or close to

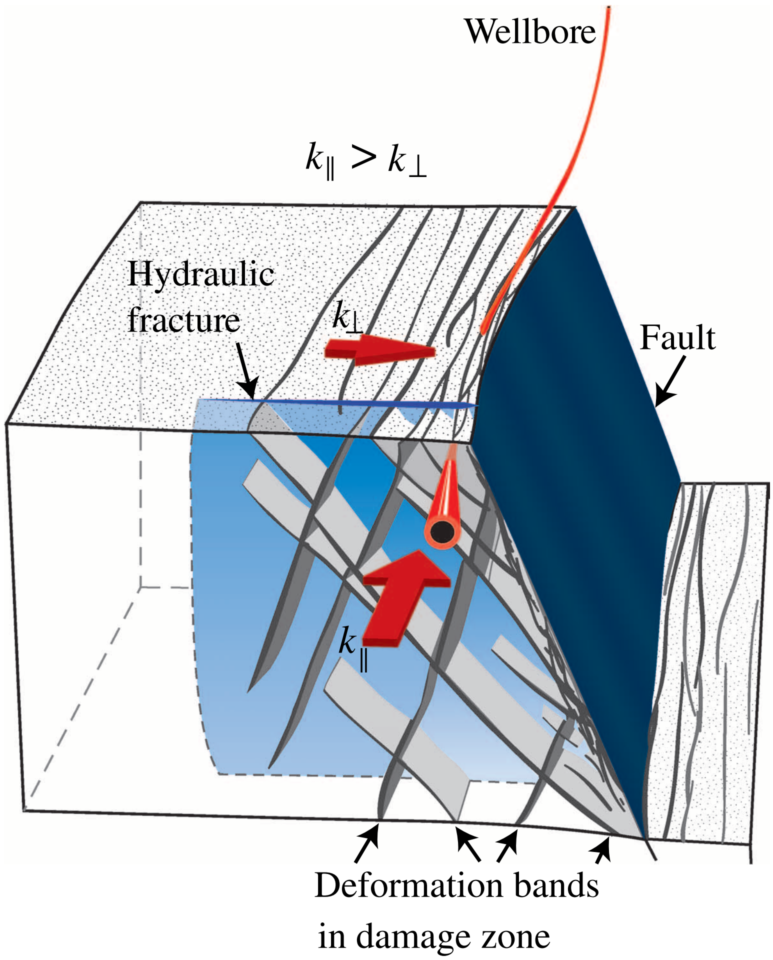

Figure 12. Schematic illustration of the typical arrangement of deformation bands in the damage zone around a simple fault. The average permeability parallel to the fault is higher than that perpendicular to the fault (red arrows) because of the arrangement of the deformation bands.

the fault in a narrow but outstretched reservoir (Dake, 1994). Thus, in theory, an unknown sealing fault located in the middle of a symmetric reservoir, and thus dividing the reservoir in two equal or separate blocks, will reduce the presumed productivity or injectivity of a centralized vertical well by 50%. Hence, poor productivity or injectivity can be explained or occasioned by other and more obvious reasons than deformation bands.

We do not deny that there may be cases where low-permeability deformation bands occur in numbers and orientations high enough that well performance is noticeably reduced. In such cases, productivity may be improved by hydraulic fracturing. Such well stimulation causes a vertical extension fracture to open. Once propped, the fracture stays open and provides a bridge across the damage zone, linking the well to pristine reservoir rock (Figure 12). Deformation bands are too thin to absorb or host any stress beyond that of the host rock. Therefore, clusters of deformation bands will not impede fracture propagation during well stimulation. Thus, hydraulic fracturing of a damage zone containing deformation bands is not different than fracturing for removal of production- or drilling-imposed damage around the wellbore. Hydraulic fracturing works because deformation bands commonly come in zones of limited thickness, thinner than the length of extension fractures generated during hydraulic fracturing.

Notably, a hydraulic fracture will always run perpendicular to the least principal stress once the fracture has propagated a few wellbore diameters from the hole. Hence, the orientation of the hydraulic fracture depends on the stress field. If the minimum principal stress is oriented perpendicular to the fault, the hydraulic fracture will run parallel to the fault and not cut through its damage zone. In this scenario, the fracture will have no effect on fluid flow across the deformation bands if the bands strike parallel to the fault. However, stress perturbation commonly occurs around faults (Dyer, 1988; Maerten et al., 2002) and may cause the hydraulic fracture to grow at an angle to the fault damage zone even for cases where the far-field minimum principal stress is perpendicular to the zone.

CONCLUSIONS

The function of deformation bands in reservoir performance is likely to be small or negligible in most cases. We base this conclusion on the following:

1. Mathematical considerations indicate that their associated reduction in permeability must be very high ($k/k_{DB} > 10^4$) and/or must occur in higher numbers than are commonly encountered in most sandstone reservoirs before representing a significant impediment to fluid flow.
2. Field observations show that they do not maintain the permeability structure and thickness along strike and dip that is inferred from core examinations and plug permeability measurements.
3. Their limited three-dimensional interconnectivity additionally reduces their function as fluid-flow baffles.

We do not claim that deformation bands cannot have any effect on fluid flow. Although they are unlikely to maintain any significant pressure difference within the reservoir, they may influence the flow pattern and reduce the sweep efficiency during injection and production in some reservoirs. This effect depends not only on the abundance and petrophysical conditions of the bands, but also on the arrangement of deformation bands in each case (Manzocchi et al., 1998). Because information about deformation-band arrangement is scarce or unavailable in most oil fields, general knowledge of deformation bands, being more or less strike parallel with associated faults, can be used to evaluate their effect in this respect. In cases where deformation-band damage zones or deformation-band clusters within the reservoir are suspected to reduce productivity or injectivity, hydraulic fracturing is likely to improve communication across the zone of deformation bands.

APPENDIX 1: CALCULATION OF LINEAR FLOW OF AN INCOMPRESSIBLE FLUID IN A LINEAR POROUS MEDIUM WITH HOMOGENEOUS FORMATION PERMEABILITY

The differential form of Darcy's law is given by

$$\frac{q}{A} = -\frac{k}{\mu}\frac{dp}{dl} \qquad (2)$$

where A is the cross sectional area, q is the flow rate, k is the permeability, μ is the viscosity, and dp/dl is the pressure gradient measured in the direction of flow. The minus sign appears in the equation because the pressure gradient is negative in the direction of flow.

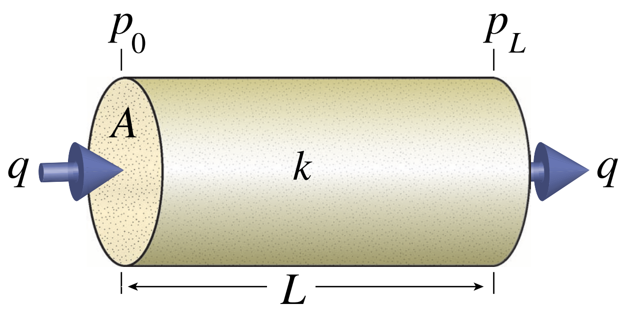

Figure 13. Linear flow through porous and homogeneous sandstone of permeability k.

Equation 2 is completely general and can be used to develop equations that pertain to many steady-state and pseudo–steady-state fluid-flow problems. Steady-state flow is where the flow rate and pressure distribution remain constant with time. In Appendices 1 and 2, we will only develop equations for steady-state, linear, and incompressible flow in porous media. The development of equations for unsteady or pseudo–steady-state flow, which is more complex, does not pertain to cases where water or gas injection represents an effective reservoir pressure maintenance scheme. Anyhow, the difference between these two flow systems will be minor in this context. The development of equations for radial flow in porous media is irrelevant for calculations of flow across lateral barriers in reservoirs hampered by deformation-band clusters parallel to major faults.

Figure 13 depicts a linear flow system with a constant cross section to flow (A) and a finite length (L). The medium has a uniform permeability (k) and is saturated with an incompressible fluid having a constant viscosity (μ). Because the fluid is incompressible, the flow rate (q) is constant at any point along the system.

We can write equation 2 with one of the variables on each side:

$$\frac{q}{A}dl = -\frac{k}{\mu}dp \qquad (3)$$

Equation 3 can be expressed in the form

$$\frac{q}{A}\int_0^L dl = -\frac{k}{\mu}\int_{p_0}^{p_L} dp \qquad (4)$$

by integrating both sides over the entire length of the medium and keeping the constants q, A, k, and μ outside the integral. Thus, equation 4 can be replaced by the identity

$$\frac{q}{A} = (L-0) = -\frac{k}{\mu}(p_L - p_0) \qquad (5)$$

Solving for q gives

$$q = \frac{kA(p_0 - p_L)}{\mu L} \qquad (6)$$

which represents the flow equation for flow of an incompressible fluid in a linear porous medium.

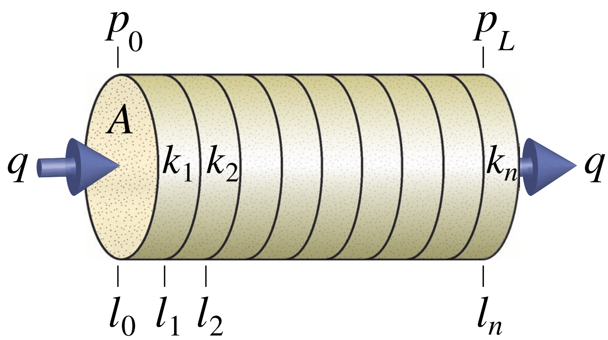

Figure 14. Linear flow through porous and heterogeneous sandstone consisting of segments (deformation bands and host rock) of individual permeabilities k_n.

APPENDIX 2: CALCULATION OF REDUCED FORMATION PERMEABILITY AS A CONSEQUENCE OF LATERAL HETEROGENEITIES SUCH AS DEFORMATION-BAND CLUSTERS AND BANDS IN DAMAGE ZONES

Figure 14 depicts a linear flow system that consists of homogeneous segments placed in series. Each segment has a permeability that may differ from that of any other segment. The points of permeability change are designated as l_0, l_1, l_2, ... l_n.

The differential form of the steady-state Darcy equation, equation 2, can be used to obtain the average permeability for a series of segments. Rearranging equation 2 with k not being a constant but a function of l and designating our integration limits give the form

$$q\int_0^L \frac{\mathrm{d}l}{k_i} = -\frac{A}{\mu}\int_{p_0}^{p_L} \mathrm{d}p \qquad (7)$$

The integral on the left side can be made more manageable by breaking the total integral into parts and integrating each part separately:

$$\int_0^L \frac{\mathrm{d}l}{k_i} = \sum_{i=1}^{n} \frac{1}{k_i}\int_{l_{i-1}}^{l_i} \mathrm{d}l = \sum_{i=1}^{n} \frac{l_i - l_{i-1}}{k_i} \qquad (8)$$

Thus, the integrated form of equation 7 is

$$q\sum_{i=1}^{n} \frac{l_i - l_{i-1}}{k_i} = -\frac{A}{\mu}(p_L - p_0) \qquad (9)$$

or solving for q,

$$q = -\frac{A(p_L - p_0)}{\mu \sum_{i=1}^{n} \frac{l_i - l_{i-1}}{k_i}} \qquad (10)$$

By comparing equation 10 with equation 6, where permeability was constant over the total length of the system, the average permeability, k_A, can be shown to be determined by the identity

$$k_A = \frac{L}{\sum_{i=1}^{n} \frac{l_i - l_{i-1}}{k_i}} \qquad (11)$$

Equation 11 implies that the average permeability, k_A, for a series of linear segments with different permeabilities, is calculated first by taking the length of every homogeneous segment and dividing by its permeability and then summing up these values for all segments. Finally, this sum is then divided into the total length of the system, L.

The reduction in flow rate or flow efficiency, FE, as a consequence of introducing lateral changes or flow impediments can be extracted by k_A/k, where k_A and k are calculated by equation 11 and equation 6, respectively.

REFERENCES CITED

Antonellini, M., and A. Aydin, 1994, Effect of faulting on fluid flow in porous sandstones: Petrophysical properties: AAPG Bulletin, v. 78, p. 355–377.

Antonellini, M. A., A. Aydin, and L. Orr, 1999, Outcrop aided characterization of a faulted hydrocarbon reservoir: Arroyo Grande oil field, California, U.S.A., *in* W. C. Haneberg, P. S. Mozley, C. J. Moore, and L. B. Goodwin, eds., Faults and subsurface fluid flow: American Geophysical Union Geophysical Monographs, v. 113, p. 7–26.

Aydin, A., and A. M. Johnson, 1978, Development of faults as zones of deformation bands and as slip surfaces in sandstones: Pure and Applied Geophysics, v. 116, p. 931–942.

Bale, A., L. Larsen, D. T. Barton, and A. Buchanan, 2001, Propped fracturing as a tool for prevention and removal of formation damage: Society of Petroleum Engineers European Formation Damage Conference, The Hague, May 21–22, 2001, SPE Paper 68913, p. 4–6.

Beitler, B., M. A. Chan, and W. T. Parry, 2003, Bleaching of Jurassic Navajo Sandstone on Colorado Plateau Laramide highs: Evidence of exhumed hydrocarbon supergiants?: Geology, v. 31, p. 1041–1044.

Billings, M. P., 1972, Structural geology, 3d ed.: Englewood Cliffs, New Jersey, Prentice Hall, 606 p.

Caine, J. S., J. P. Evans, and C. B. Forster, 1996, Fault zone architecture and permeability structure: Geology, v. 24, p. 1025–1028.

Chan, M. A., W. T. Parry, and J. R. Bowman, 2000, Diagenetic hematite and manganese oxides and fault-related fluid flow in Jurassic sandstones, southeastern Utah: AAPG Bulletin, v. 84, p. 1281–1310.

Chan, M. A., W. T. Parry, E. U. Petersen, and C. M. Hall, 2001, $^{40}Ar/^{39}Ar$ age and chemistry of manganese mineralization in the Moab and Lisbon fault systems, southeastern Utah: Geology, v. 29, p. 331–334.

Crawford, B. R., 1998, Experimental fault sealing: Shear band permeability dependency on cataclastic fault gouge characteristics, *in* M. P. Coward, H. Johnson, and T. S. Daltaban, eds., Structural geology in reservoir characterization: Geological Society (London) Special Publication 127, p. 83–97.

Dake, L. P., 1994, The practice of reservoir engineering: Amsterdam, Elsevier, 534 p.

Dietz, D. N., 1965, Determination of average reservoir pressure from buildup surveys: Journal of Petroleum Technology, v. 234, p. 955–959.

Du Bernard, X., P. Eichhubl, and A. Aydin, 2002, Dilation bands: A new form of localized failure in granular media: Geophysical Research Letters, v. 29, p. 2176–2179.

Dyer, R., 1988, Using joint interactions to estimate paleostress ratios: Journal of Structural Geology, v. 10, p. 685–699.

Eichhubl, P., W. L. Taylor, D. D. Pollard, and A. Aydin, 2004, Paleo-fluid flow and deformation in the Aztec Sandstone at the

Valley of Fire, Nevada— Evidence for the coupling of hydrogeologic, diagenetic, and tectonic processes: Geological Society of America Bulletin, v. 116, p. 1120–1136.
Fisher, Q. J., and R. J. Knipe, 2001, The permeability of faults within siliciclastic petroleum reservoirs of the North Sea and Norwegian continental shelf: Marine and Petroleum Geology, v. 18, p. 1063–1081.
Flodin, E. A., M. Gerdes, A. Aydin, and W. D. Wiggins, 2005, Petrophysical properties and sealing capacity of fault rock, Aztec Sandstone, Nevada, *in* R. Sorkhabi and Y. Tsuji, eds., Faults, fluid flow, and petroleum traps: AAPG Memoir 85, p. 197–217.
Fossen, H., and J. Hesthammer, 1997, Geometric analysis and scaling relations of deformation bands in porous sandstone: Journal of Structural Geology, v. 19, p. 1479–1493.
Fossen, H., S. E. Johansen, J. Hesthammer, and A. Rotevatn, 2005, Fault interaction in porous sandstone and implications for reservoir management; examples from southern Utah: AAPG Bulletin, v. 89, p. 1593–1606.
Fossen, H., R. A. Schulz, Z. K. Shipton, and K. Mair, 2007, Deformation bands in sandstone— A review: Geological Society (London), v. 164, p. 755–769.
Fowles, J., and S. Burley, 1994, Textural and permeability characteristics of faulted, high porosity sandstones: Marine and Petroleum Geology, v. 11, p. 608–623.
Garden, I. R., S. C. Guscott, S. D. Burley, and K. A. Foxford, 2001, An exhumed palaeo-hydrocarbon migration fairway in a faulted carrier system, Entrada Sandstone of SE Utah, U.S.A.: Geofluids, v. 1, p. 195–213.
Gibson, R. G., 1994, Fault-zone seals in siliclastic strata of the Columbus Basin, offshore Trinidad: AAPG Bulletin, v. 78, p. 1372–1385.
Gibson, R. G., 1998, Physical character and fluid-flow properties of sandstone derived fault gouge, *in* M. P. Coward, H. Johnson, and T. S. Daltaban, eds., Structural geology in reservoir characterization, Geological Society (London) Special Publication 127, p. 83–97.
Harper, T., and I. Moftah, 1985, Skin effect and completion options in the Ras Budran reservoir, *in* Society of Petroleum Engineers Middle East Oil Technical Conference and Exhibition, SPE Paper 13708, p. 211–226.
Hesthammer, J., and H. Fossen, 2001, Structural core analysis from the Gullfaks area, northern North Sea: Marine and Petroleum Geology, v. 18, p. 411–439.
Hesthammer, J., T. E. S. Johansen, and L. Watts, 2000, Spatial relationships within fault damage zones in sandstone: Marine and Petroleum Geology, v. 17, p. 873–893.
Hesthammer, J., P. A. Bjørkum, and L. I. Watts, 2002, The effect of temperature on sealing capacity of faults in sandstone reservoirs: Examples from the Gullfaks and Gullfaks Sør fields, North Sea: AAPG Bulletin, v. 86, p. 1733–1751.
Hobbs, B. E., W. D. Means, and P. F. Williams, 1976, An outline of structural geology: New York, J. Wiley and Sons, 571 p.
Jamison, W. R., and D. W. Stearns, 1982, Tectonic deformation of Wingate Sandstone, Colorado National Monument: AAPG Bulletin, v. 66, p. 2584–2608.
Johansen, S. E., and H. Fossen, in press, Internal geometry of fault damage zones in siliclastic rocks, *in* W. Kurz, C. A. J. Wibberley, J. Imber, C. Collettini, and R. E. Holdsworth, eds., The internal structure of fault zones: Fluid flow and mechanical properties: Geological Society (London) Special Publication.
Jourde, H., E. A. Flodin, A. Aydin, L. J. Durlofsky, and X. Wen, 2002, Computing permeabilities of fault zones in eolian sandstone from outcrop measurements: AAPG Bulletin, v. 86, p. 1187–1200.
Knipe, R. J., Q. J. Fisher, M. R. Clennell, A. B. Farmer, A. Harrison, B. Kidd, E. McAllister, J. R. Porter, and E. A. White, 1997, Fault seal analysis: Successful methodologies, application and future directions, *in* P. Møller-Pedersen and A. G. Koestler, eds., Hydrocarbon seals: Importance for exploration and production: Norwegian Petroleum Society (NPF) Special Publication 7, p. 15–40.
Knott, S. D., 1993, Fault seal analysis in the North Sea: AAPG Bulletin, v. 77, p. 778–792.
Knott, S. D., A. Beach, P. J. Brockbank, J. L. Brown, J. E. McCallum, and A. I. Welbon, 1996, Spatial and mechanical controls on normal fault populations: Journal of Structural Geology, v. 18, p. 359–372.
Lothe, A. E., R. H. Gabrielsen, N. Bjørnevoll-Hagen, and B. T. Larsen, 2002, An experimental study of the texture of deformation bands; effects on the porosity and permeability of sandstones: Petroleum Geoscience, v. 8, p. 195–207.
Maerten, F., P. Gillespie, and D. D. Pollard, 2002, Effects of local stress perturbation on secondary fault development: Journal of Structural Geology, v. 24, p. 145–153.
Manzocchi, T., P. S. Ringose, and J. R. Underhill, eds., 1998, Flow through fault systems in high-porosity sandstones: Structural geology in reservoir characterization: Geological Society (London) Special Publication 127, p. 65–82.
Mollema, P. N., and M. A. Antonellini, 1996, Compaction bands: A structural analog for anti-mode I cracks in aeolian sandstone: Tectonophysics, v. 267, p. 209–228.
Ogilvie, S. R., and P. W. J. Glover, 2001, The petrophysical properties of deformation bands in relation to their microstructure: Earth and Planetary Science Letters, v. 193, p. 129–142.
Peacock, D. C. P., R. J. Knipe, and D. J. Sanderson, 2000, Glossary of normal faults: Journal of Structural Geology, v. 22, p. 291–305.
Pittman, E. D., 1981, Effect of fault-related granulation on porosity and permeability of quartz sandstones, Simpson Group (Ordovician), Oklahoma: AAPG Bulletin, v. 65, p. 2381–2387.
Schultz, R. A., and H. Fossen, 2002, Displacement-length scaling in three dimensions: The importance of aspect ratio and application to deformation bands: Journal of Structural Geology, v. 24, p. 1389–1411.
Shipton, Z. K., and P. Cowie, 2003, A conceptual model for the origin of fault damage zone structures in high-porosity sandstone: Journal of Structural Geology, v. 25, p. 333–344.
Shipton, Z. K., J. P. Evans, K. Robeson, C. B. Forster, and S. Snelgrove, 2002, Structural heterogeneity and permeability in faulted aeolian sandstone: Implications for subsurface modelling of faults: AAPG Bulletin, v. 86, p. 863–883.
Shipton, Z. K., J. P. Evans, and L. B. Thompson, 2005, The geometry and thickness of deformation-band fault core and its influence on sealing characteristics of deformation-band fault zones: AAPG Memoir, v. 85, p. 181–195.
Sigda, J. M., L. B. Goodwin, P. S. Mozley, and J. L. Wilson, 1999, Permeability alteration in small-displacement faults in poorly lithified sediments: Rio Grande rift, central New Mexico: Geophysical Monograph, v. 113, p. 51–68.
Solum, J. G., B. van der Pluijm, and D. R. Peacor, 2005, Neocrystallization, fabrics and age of clay, minerals from an exposure of the Moab fault, Utah: Journal of Structural Geology, v. 27, p. 1563–1576.
Taylor, W. L., and D. D. Pollard, 2000, Estimation of in situ permeability of deformation in porous sandstone, Valley of Fire, Nevada: Water Resources Research, v. 36, p. 2595–2606.
Walderhaug, O., 1996, Kinetic modeling of quartz cementation and porosity loss in deeply buried sandstone reservoirs: AAPG Bulletin, v. 80, p. 731–745.
Walsh, J. J., J. Watterson, A. E. Heath, and C. Childs, 1998, Representation and scaling of faults in fluid flow models: Petroleum Geoscience, v. 4, p. 241–251.